Journal of Thermal Analysis, Vol. 48 (1997) 207-224

MODELING THE HEAT FLOW AND HEAT CAPACITY OF MODULATED DIFFERENTIAL SCANNING CALORIMETRY

B. Wunderlich

Department of Chemistry, The University of Tennessee, Knoxville, TN 37996–1600
and Chemistry and Analytical Sciences, Division, Oak Ridge National Laboratory, Oak Ridge, TN 37831–6197, USA

(Received February 23, 1996)

Abstract

Modulated differential scanning calorimetry (MDSC) uses an abbreviated Fourier transformation for the data analysis and separation of the reversing component of the heat flow and temperature signals. In this paper a simple spread-sheet analysis will be presented that can be used to better understand and explore the effects observed in MDSC and their link to actual changes in the instrument and sample. The analysis assumes that instrument lags and other kinetic effects are either avoided or corrected for.

Keywords: calorimetry, Fourier series, heat capacity, heat flow calorimeter, MDSC, spread-sheet analysis, temperature modulated calorimetry

Introduction

Modulated differential scanning calorimetry, MDSC, [1] is based on temperature modulation and has recently also been called TMDSC [2]. The treatment in this paper uses the formalism developed for heat-flux calorimetry, as can be carried out with the TA Instruments MDSC 2920. In prior publications from our laboratory we have given a general mathematical description of MDSC [3], discussed a method of quasi-isothermal MDSC for heat capacity measurement with the necessary calibration instructions and limits for producing high-quality data [4], addressed the questions of linearity, steady state, and complex heat capacity [5], and explored the time dependence of the heat capacity as experienced in the glass transition region [6–8]. A general, computer-generated lecture course on MDSC was produced, and is available through the World Wide Web [9].

In this paper a simple method is developed to explore the link between the recorded heat capacity or heat flow as given by the software of the MDSC and the assumed and modelled changes within the calorimeter and sample. A simple spread sheet, as is available in any personal computer, is used for the computation and plotting. The basic program is set up in Lotus 1–2–3™ (Release 4 for Windows™), but any other spread sheets should work as well. The actual worked-out

0368–4466/97/ $ 5.00

John Wiley & Sons Limited
Chichester

spread sheet can be downloaded from our WWW home page [9] and easily modified to any specific application. Note that this analysis assumes that the calorimetric signal contains only negligible instrument lag, i.e. the always present lag is within the limits explored earlier [5], or it is corrected for. In either case, this analysis is then suitable to directly convert a modelled kinetics of a chemical or physical process to the expected output from an MDSC measurement for comparison of model and experiment. Detailed models for the kinetics of the glass transition that can be fed directly into the here presented spread-sheet are presently tested and will be published in due time [7, 8]. With minor modification it is also possible to use the present spread-sheet to convert the result of a kinetics model to the expected signal of a Mettler ADSC or a Perkin-Elmer DDSC (again under the condition that instrument effects have been eliminated). Naturally it is also possible to judge the quality of the various modulation equipment by a comparison of the modelled output of a process used for calibration with the actual calorimeter output. As can be seen from the displayed figures, reversible, total, and irreversible signals are computed.

Modulated calorimetry

In MDSC a simple, sinusoidal modulation changes the increasing block temperature $T_b(t)$ to:

$$T_b(t) = T_o + \langle q \rangle t + A_{T_b} \sin(\omega t) \tag{1}$$

where $\langle q \rangle$ is the underlying heating rate, obtained by forming a running average over two complete modulation periods; and ω, the modulation frequency $2\pi/p$, with p representing the period of one cycle in seconds. The amplitude A_{T_b} at the heater block is adjusted such that a preset amplitude A is observed at the sample position. For this reason, one needs only to discuss the response to this modulation in the temperature difference between reference and sample thermocouple $\Delta T = T_r - T_s$. The heat flow HF given in J s^{-1} or watts is proportional to this temperature difference, given in kelvins. Typical temperature modulations may have a maximum amplitude A between 0.1 and 2 K and a period between 10 and 100 s. The condition for quantitative measurement is a negligible temperature gradient within the sample and continuous steady state [5, 6, 10]. Limits to the actual run parameters were established earlier [4].

The approach to steady state of the change in temperature as a function of time can be judged, for example, at the sample position of the calorimeter, $T_s(t)$, and is given by [4]:

$$\begin{aligned} T_s(t) - T_o - \langle q \rangle t = -\langle q \rangle \frac{C_s}{K}(1 - e^{-Kt/C_s}) + \\ + A[\cos\varepsilon \sin\omega t - \sin\varepsilon \cos\omega t + \sin\varepsilon\, e^{-Kt/C_s}] \end{aligned} \tag{2}$$

where T_o, is the temperature at the start of the experiment; C_s, the heat capacity of the sample calorimeter (consisting of sample and pan); K, the Newton's law con-

stant governing the heat flow; and ε is the phase shift relative to the modulation frequency ω at the block and is given by:

$$\sin\varepsilon = \frac{\omega}{\sqrt{(K/C_s)^2 + \omega^2}} \tag{3}$$

The trigonometric addition theorem $\cos\varepsilon \sin\omega t - \sin\varepsilon \cos\omega t = \sin(\omega t - \varepsilon)$ can be used to condense Eq. (2), and the equation $\sin^2\varepsilon + \cos^2\varepsilon = 1$ permits evaluation of $\cos\varepsilon$ from Eq. (3). Steady state is reached as soon as all terms with the factor e^{-Kt/C_s} become negligible:

$$T_s(t) - T_o - \langle q \rangle t = -\langle q \rangle \frac{C_s}{K} + A \sin(\omega t - \varepsilon) \tag{4}$$

Analogous equations hold for the reference temperature (phase shift φ) and the temperature difference, ΔT (phase shift δ) [3]. Evaluation of qC_s/K without the modulation influence leads to the standard DSC result and is duplicated, as shown below, by the 'total heat flow' ($\langle HF(t) \rangle$). Determination of the calibration constants, measurement of A_Δ or A_{HF}, and setting of the modulation amplitude A of T_s and the modulation frequency ω allow, then, to determine the heat capacity in a second mode from the modulation alone (determination of the 'reversing' heat capacity):

$$mc_p = \frac{A_\Delta}{A} \sqrt{(K/\omega)^2 + C'^2} = \frac{A_{HF}}{A} K' \tag{5}$$

where m is the sample mass; c_p, the specific heat capacity of the sample; and C', the heat capacity of the empty reference pan of identical mass to the empty sample pan. The calibration constant K is independent of modulation frequency and reference heat capacity. The commonly measured calibration constant K' changes for runs with different ω and C'.

Modeling of the software deconvolution of the measurement

The deconvolution of the heat flow signal in MDSC, needed for the evaluation of Eq. (5) is a running, real-time process that examines *three* modulation periods of input for each point generated when using the software supplied with the TA Instruments MDSC 2910 or 2920. The output is the appropriately smoothed average, computed for the measurement made 1.5 periods earlier. The on-line data recording lags for this reason 1.5 cycles behind the measurement, and one may have to make adjustments when comparing smoothed values and instantaneous data.

For clarity, seven times are defined in this discussion for the generation of one data point:

$$t_o \ldots t_n \ldots t_6 = t_o - (n/2)p$$

(note that in MDSC time is counted backwards from the last point considered at t_o, to the first point needed for computation t_6).

In the example spread sheet of Table 1 the first column contains a listing of the time, t, in steps of two seconds. To save space, only half the spread sheet is printed. The present, simple spread sheet covers the time from 0 to 200 s. The period p was assumed to be 100 s (frequency 0.01 Hz), so that $t_0=0$ s, $t_1=50$ s, $t_2=100$ s, $t_3=150$ s, and $t_6=300$ s. The second column is a listing of the assumed instantaneous heat flow $HF(t)$. In Table 1 it is simply taken to be $1.0+1.0\times\sin(\omega t-\pi/4)$. This corresponds to heat capacity difference between sample and reference causing a heat flow of 1.00 at the chosen underlying heating rate $<q>$, and a sinusoidally modulated temperature that causes a phase angle δ of $\pi/4$ in the temperature difference, and a maximum heat flow amplitude A_{HF} of 1.00. These values are chosen for convenience of computation and do not represent actual data or DSC cell properties. Figure 1 shows $HF(t)$ as the phase-shifted sinusoidal curve (heavy curve), clearly indicating the maximum modulation amplitude of 1.0 and the additional constant heat flow contribution from the underlying heating rate $<q>$ which is also 1.0.

For analysis the heat flow is conveniently expressed as a Fourier series, as can be found in any text on the subject, including the derivation of the recursion formulas:

$$HF(t) = b_0 + \sum_{\nu=1}^{\nu=\infty}\left[a_\nu \sin\frac{2\pi\nu}{p}t + b_\nu \cos\frac{2\pi\nu}{p}t\right] \tag{6}$$

with the constant b_0 and the maximum amplitudes a_ν and b_ν, given by:

$$b_0 = \frac{1}{p}\int_{-p/2}^{+p/2} HF(t)\,dt \tag{7}$$

$$a_\nu = \frac{1}{2p}\int_{-p/2}^{+p/2} HF(t)\sin\left(\frac{2\pi\nu}{p}t\right)dt \tag{8}$$

$$b_\nu = \frac{1}{2p}\int_{-p/2}^{+p/2} HF(t)\cos\left(\frac{2\pi\nu}{p}t\right)dt \tag{9}$$

where ν is a running integer starting from 1.

The deconvolution starts with the evaluation of b_0, which is called the *total heat flow* $<HF(t)>$ in the generally accepted nomenclature of MDSC. The integration in Eq. (7) is replaced by the sum in the steps of 2 s of the spread sheet (note that the MDSC can evaluate the heat flow every 0.2 s and produces thus in its sum an even closer match to the integral):

$$<HF(t)> = \frac{\sum_{t-50}^{t+50} HF(t) - 1/2HF(t-50) - 1/2HF(t+50)}{50} \tag{10}$$

Table 1 Sample spread sheet for modulation and underlying heating rate

Time/s	*HF*(*t*)	*HF*(corr)	*HF*(cos)	*HF*(sin)	<*HF*(cos)>	<*HF*(sin)>	<*A*(*HF*)>	<*A*(*HF*)> smooth
0	0.292893							
2	0.387093							
4	0.490959							
6	0.602852							
8	0.721009							
10	0.843566							
12	0.968589							
14	1.094108							
16	1.218143							
18	1.338738							
20	1.45399							
22	1.562083							
24	1.661312							
26	1.750111							
28	1.827081							
30	1.891007							
32	1.940881							
34	1.975917							
36	1.995562							
38	1.999507							
40	1.987688							

Table 1 Continued

Time /s	*HF*(*t*)	*HF*(corr)	*HF*(cos)	*HF*(sin)	<*HF*(cos)>	<*HF*(sin)>	<*A*(*HF*)>	<*A*(*HF*)> smooth
42	1.960294							
44	1.917755							
46	1.860742							
48	1.790155							
50	1.707107	0.707107	–0.70711	1.1E–19				
52	1.612907	0.612907	–0.60807	–0.07682				
54	1.509041	0.509041	–0.49305	–0.12659				
56	1.397148	0.397148	–0.36926	–0.1462				
58	1.278991	0.278991	–0.24448	–0.1344				
60	1.156434	0.156434	–0.12656	–0.09195				
62	1.031411	0.031411	–0.0229	–0.0215				
64	0.905892	–0.09411	0.059987	0.072512				
66	0.781857	–0.21814	0.116887	0.184184				
68	0.661262	–0.33874	0.144228	0.306499				
70	0.54601	–0.45399	0.140291	0.431771				
72	0.437917	–0.56208	0.105324	0.552127				
74	0.338688	–0.66131	0.041524	0.660007				
76	0.249889	–0.75011	–0.0471	0.748631				
78	0.172919	–0.82708	–0.15498	0.812431				
80	0.108993	–0.89101	–0.27534	0.847398				
82	0.059119	–0.94088	–0.40061	0.851334				

Table 1 Continued

Time/s	*HF*(*t*)	*HF*(corr)	*HF*(cos)	*HF*(sin)	<*HF*(cos)>	<*HF*(sin)>	<*A*(*HF*)>	<*A*(*HF*)> smooth
84	0.024083	–0.97592	–0.52292	0.823994				
86	0.004438	–0.99556	–0.6346	0.767094				
88	0.000493	–0.99951	–0.72861	0.684209				
90	0.012312	–0.98769	–0.79906	0.580549				
92	0.039706	–0.96029	–0.84151	0.462625				
94	0.082245	–0.91775	–0.85331	0.337848				
96	0.139258	–0.86074	–0.8337	0.214058				
98	0.209845	–0.79016	–0.78392	0.099033				
100	0.292893	–0.70711	–0.70711	2.3E–19	–0.35355	0.353553	1	
102	0.387093	–0.61291	–0.60807	–0.07682	–0.35355	0.353553	1	
104	0.490959	–0.50904	–0.49305	–0.12659	–0.35355	0.353553	1	
106	0.602852	–0.39715	–0.36926	–0.1462	–0.35355	0.353553	1	
108	0.721009	–0.27899	–0.24448	–0.1344	–0.35355	0.353553	1	
110	0.843566	–0.15643	–0.12656	–0.09195	–0.35355	0.353553	1	
112	0.968589	–0.03141	–0.0229	–0.0215	–0.35355	0.353553	1	
114	1.094108	0.094108	0.059987	0.072512	–0.35355	0.353553	1	
116	1.218143	0.218143	0.116887	0.184184	–0.35355	0.353553	1	
118	1.338738	0.338738	0.144228	0.306499	–0.35355	0.353553	1	
120	1.45399	0.45399	0.140291	0.431771	–0.35355	0.353553	1	
122	1.562083	0.562083	0.105324	0.552127	–0.35355	0.353553	1	
124	1.661312	0.661312	0.041524	0.660007	–0.35355	0.353553	1	

Table 1 Continued

Time/s	*HF*(*t*)	*HF*(corr)	*HF*(cos)	*HF*(sin)	<*HF*(cos)>	<*HF*(sin)>	<*A*(*HF*)>	<*A*(*HF*)> smooth
126	1.750111	0.750111	–0.0471	0.748631	–0.35355	0.353553	1	
128	1.827081	0.827081	–0.15498	0.812431	–0.35355	0.353553	1	
130	1.891007	0.891007	–0.27534	0.847398	–0.35355	0.353553	1	
132	1.940881	0.940881	–0.40061	0.851334	–0.35355	0.353553	1	
134	1.975917	0.975917	–0.52292	0.823994	–0.35355	0.353553	1	
136	1.995562	0.995562	–0.6346	0.767094	–0.35355	0.353553	1	
138	1.999507	0.999507	–0.72861	0.684209	–0.35355	0.353553	1	
140	1.987688	0.987688	–0.79906	0.580549	–0.35355	0.353553	1	
142	1.960294	0.960294	–0.84151	0.462625	–0.35355	0.353553	1	
144	1.917755	0.917755	–0.85331	0.337848	–0.35355	0.353553	1	
146	1.860742	0.860742	–0.8337	0.214058	–0.35355	0.353553	1	
148	1.790155	0.790155	–0.78392	0.099033	–0.35355	0.353553	1	
150	1.707107	0.707107	–0.70711	3.4E–19	–0.35355	0.353553	1	1
152	1.612907	0.612907	–0.60807	–0.07682	–0.35355	0.353553	1	1
154	1.509041	0.509041	–0.49305	–0.12659	–0.35355	0.353553	1	1
156	1.397148	0.397148	–0.36926	–0.1462	–0.35355	0.353553	1	1
158	1.278991	0.278991	–0.24448	–0.1344	–0.35355	0.353553	1	1
160	1.156434	0.156434	–0.12656	–0.09195	–0.35355	0.353553	1	1
162	1.031411	0.031411	–0.0229	–0.0215	–0.35355	0.353553	1	1
164	0.905892	–0.09411	0.059987	0.072512	–0.35355	0.353553	1	1
166	0.781857	–0.21814	0.116887	0.184184	–0.35355	0.353553	1	1

Table 1 Continued

Time/s	*HF*(*t*)	*HF*(corr)	*HF*(cos)	*HF*(sin)	<*HF*(cos)>	<*HF*(sin)>	<*A*(*HF*)>	<*A*(*HF*)> smooth
168	0.661262	–0.33874	0.144228	0.306499	–0.35355	0.353553	1	1
170	0.54601	–0.45399	0.140291	0.431771	–0.35355	0.353553	1	1
172	0.437917	–0.56208	0.105324	0.552127	–0.35355	0.353553	1	1
174	0.338688	–0.66131	0.041524	0.660007	–0.35355	0.353553	1	1
176	0.249889	–0.75011	–0.0471	0.748631	–0.35355	0.353553	1	1
178	0.172919	–0.82708	–0.15498	0.812431	–0.35355	0.353553	1	1
180	0.108993	–0.89101	–0.27534	0.847398	–0.35355	0.353553	1	1
182	0.059119	–0.94088	–0.40061	0.851334	–0.35355	0.353553	1	1
184	0.024083	–0.97592	–0.52292	0.823994	–0.35355	0.353553	1	1
186	0.004438	–0.99556	–0.6346	0.767094	–0.35355	0.353553	1	1
188	0.000493	–0.99951	–0.72861	0.684209	–0.35355	0.353553	1	1
190	0.012312	–0.98769	–0.79906	0.580549	–0.35355	0.353553	1	1
192	0.039706	–0.96029	–0.84151	0.462625	–0.35355	0.353553	1	1
194	0.082245	–0.91775	–0.85331	0.337848	–0.35355	0.353553	1	1
196	0.139258	–0.86074	–0.8337	0.214058	–0.35355	0.353553	1	1
198	0.209845	–0.79016	–0.78392	0.099033	–0.35355	0.353553	1	1
200	0.292893	–0.70711	–0.70711	4.6E–19	–0.35355	0.353553	1	1

The total heat flow is, thus, the same as would have been measured without modulation by standard DSC (as long as the conditions for MDSC and DSC are fulfilled, namely, negligible temperature gradient within the sample and steady state). The first time at which $\langle HF(t)\rangle$ can be determined is at $t_1 = 50$ s.

For the further description of the heat flow, one realizes that one can conveniently rewrite the Fourier series of Eq. (6) in terms of $HF(\text{corr}) = HF(t) - \langle HF(t)\rangle$. In this case b_0 is included on the left-hand side of Eq. (6) and the analysis is that of what can be called a pseudo-isothermal case. The effect of the underlying heating rate is separated from the further analysis. It will be shown below to what degree this separation is valid. The values for $HF(\text{corr})$ are listed in the third column of Table 1 [=Column 2 – Eq. (10)]. One can furthermore recognize, that for the strictly sinusoidal modulation only terms with a_1 and b_1 in the Fourier series need be considered.

Columns four and five of Table 1 are computed next as:

$$HF_{\sin}(t) = HF(\text{corr}) \times \sin\omega t \; t \geq 50 \text{ s} \quad [= A_{HF}\sin(\omega t - \delta)\sin\omega t] \tag{11}$$

$$HF_{\cos}(t) = HF(\text{corr}) \times \cos\omega t \; t \geq 50 \text{ s} \quad [= A_{HF}\sin(\omega t - \delta)\cos\omega t] \tag{12}$$

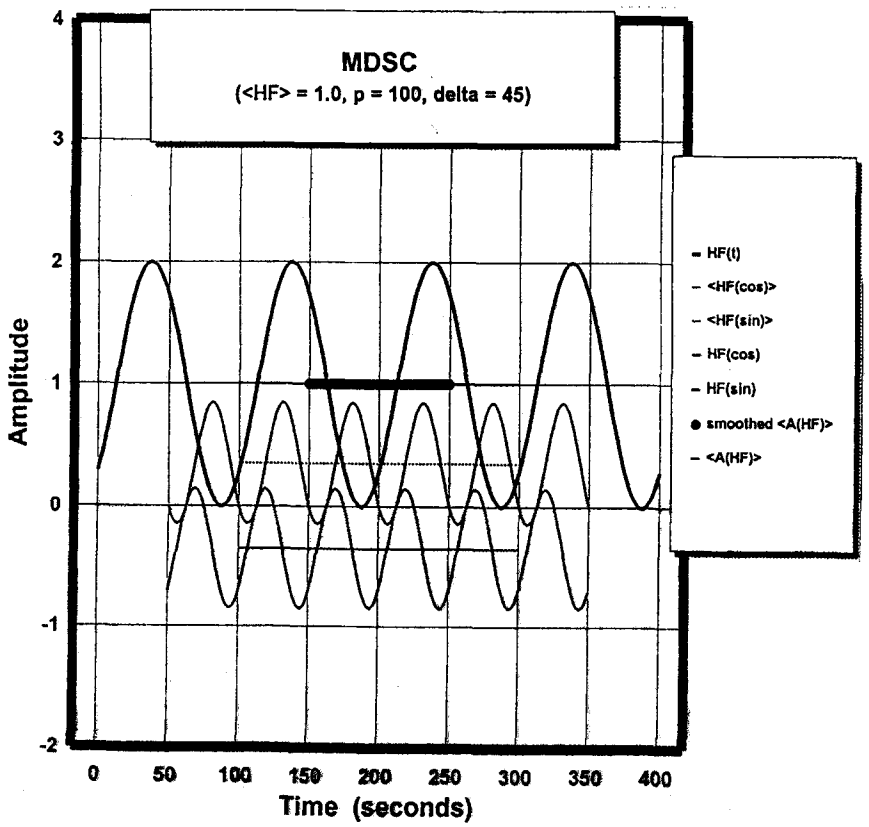

Fig. 1 Spread-sheet simulation of an MDSC experiment

They represent the integrands of a_1 and b_1, as expressed in Eqs (8) and (9), respectively. The middle sinusoidal curve in Fig. 1 represents Eq. (11) and the lower one Eq. (12). The terms in brackets give the functional relationship for the two integrands to the amplitude of the heat flow $HF(t)$, as given in the upper sinusoidal curve.

To evaluate a_1 and b_1 one can, again, average over the full period, p, instead of carrying out the integration, as is shown in columns six and seven of Table 1 and indicated in Fig. 1 by the dotted horizontals. The Fourier coefficients can now be written in the MDSC nomenclature as $a_1=2\langle HF_{sin}(t)\rangle$ and $b_1= 2\langle HF_{cos}(t)\rangle$:

$$\langle HF_{sin}(t)\rangle = \frac{\sum_{t-50}^{t+50} HF_{sin}(t) - 1/2HF_{sin}(t-50) - 1/2HF_{sin}(t+50)}{50} \qquad (13)$$

$$[= \langle (A_{HF}/2)\cos\delta \rangle]$$

$$\langle HF_{cos}(t)\rangle = \frac{\sum_{t-50}^{t+50} HF_{cos}(t) - 1/2HF_{cos}(t-50) - 1/2HF_{cos}(t+50)}{50} \qquad (14)$$

$$[= \langle (A_{HF}/2)\sin\delta \rangle]$$

Because Eq. (10) can be evaluated for the first time only at time $t_1=50$ s, Eqs (13) and (14) can be evaluated first at $t_2=100$ s (Table 1). The terms in brackets gives the integrals of the corresponding integrands in brackets in Eqs (11) and (12). For a phase shift δ of zero, $\langle HF_{sin}(t)\rangle$ is 0.5 and $\langle HF_{cos}(t)\rangle$ is 0 and for the chosen δ of Table 1 of $\pi/2$, $\langle HF_{sin}(t)\rangle$ is +0.3535 and $\langle HF_{cos}(t)\rangle$ is −0.35355, as can be easily seen from the bracketed terms in Eqs (13) and (14). Expressing the Fourier series in complex notation, Eqs (13) and (14) must be linked to the coefficient c_{+1} of the equivalent series:

$$HF(t) = \sum_{\nu=-\infty}^{+\infty} c_\nu \, e^{(2i\nu\pi/p)t} \qquad (15)$$

$$c_\nu = \frac{b_\nu + ia_\nu}{2} \quad \text{for } \nu < 0 \qquad (16)$$

$$c_\nu = \frac{b_\nu - ia_\nu}{2} \quad \text{for } \nu > 0 \qquad (17)$$

$$c_\nu = b_0 \quad \text{for } \nu = 0 \qquad (18)$$

Simple vector addition of the cosine and sine averages of Eqs (13) and (14) gives the average maximum amplitude of modulation of the heat flow:

$$<A_{HF}> = 2\sqrt{<HF_{sin}(t)>^2 + <HF_{cos}(t)>^2} \quad (19)$$

The maximum amplitude of the heat flow modulation, $<A_{HF}>$, is listed in column eight of Table 1 and is shown as the thin horizontal at 1.00. As expected, the assumed modulation of the heat-flow amplitude is recovered. The signal is further smoothed by computing the additional average given in the last column of Table 1 and drawn as the heavy line in Fig. 1:

$$<A_{HF}(t)>\text{smoothed} = \frac{\sum_{t-50}^{t+50} A_{HF}(t) - 1/2A_{HF}(t-50) - 1/2A_{HF}(t+50)}{50} \quad (20)$$

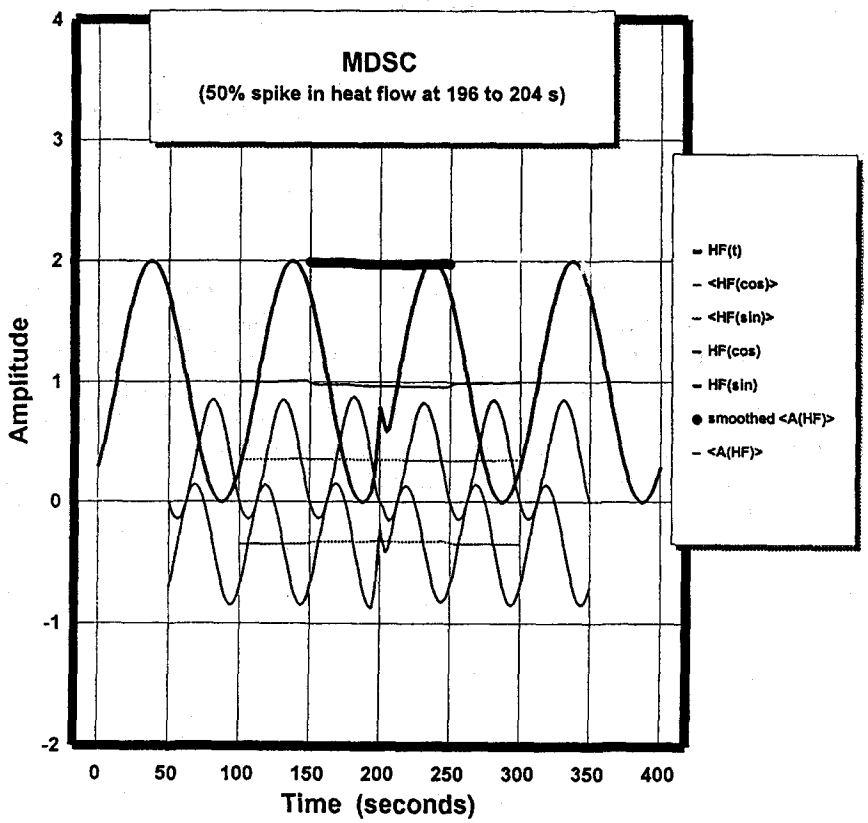

Fig. 2 Similar analysis as in Fig. 1, but with a heat-flow spike at 200 s. Note that for clarity the smoothed $<A_{HF}>$ has been moved upwards by one unit. The HF_{sin} is the middle sinusoidal curve

This further averaging postpones the first point calculated on-line after measuring to $t_3 = 150$ s.

Once set-up, this spread sheet can now easily be modified by changing column two to simulate other, more complicated experimental conditions. Changing column 1 can extend the range analyzed. For our discussion of the kinetics of the glass transition [8] up to 2500 steps have been included, to easily cover the whole transition region. The spread sheet, as just described, is available via WWW [9] as file MDSCDAT.WK4 that also includes Fig. 1. The authors are also glad to copy the file to your empty, IBM-compatibly formatted diskette.

Discussion

The detailed link of the analysis given by the MDSC software to the Fourier series of Eq. (6) shows the much greater simplicity of a sinusoidal modulation over any other function. All higher harmonics ($\nu \geq 1$) can be neglected. These higher harmonics would correspond to a higher instantaneous heating rate $q(t) = dT_s/dt$, and a

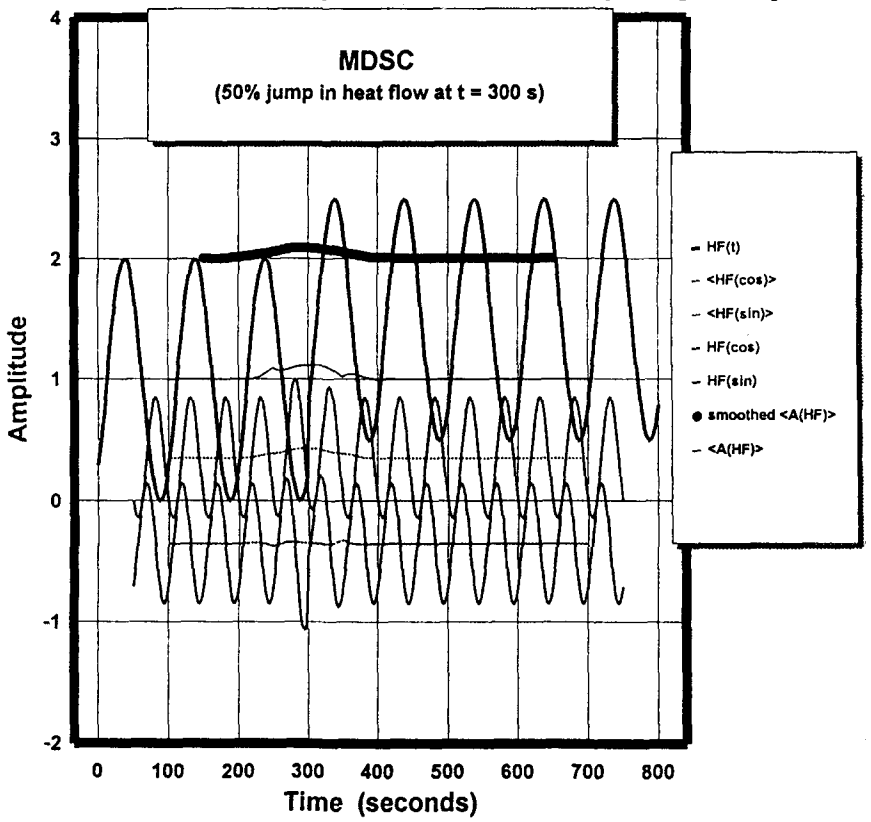

Fig. 3 Similar analysis as in Fig. 1, but with a spike in heat flow at 300 s. Note that for clarity the smoothed $\langle A_{HF} \rangle$ has been moved upwards by one unit. The HF_{sin} is the middle sinusoidal curve

loss of steady state would be more likely in case one wants to make a full evaluation of the Fourier series. For well chosen modulation functions, it may perhaps be possible to compute the required amplitudes for Eq. (4) from the first Fourier coefficients.

The question to be answered in this discussion is how typical instrument and sample effects register through the software. The first example is shown in Fig. 2. It involves the introduction of a sharp spike of a 50% increase in heat flow (column 1 of Table 1, amplitudes of 1.1, 1.3, 1.5, 1.3 and 1.1, instead of 1.0 at 196, 198, 200, 202 and 204 s, respectively). This is a major effect in a DSC trace. A smaller spike of this nature could represent an error caused by mechanical movement of the sample or reference, a break in the gas flow, or other similar systematic errors. A larger spike of this nature may signal a transition with a latent heat.

Inspection of Fig. 2 shows that the spike is smoothed over the full three cycles involved in the various averages and given an overall negative heat-flow contribution despite of its positive value. Inspecting the spread sheet and experimentation

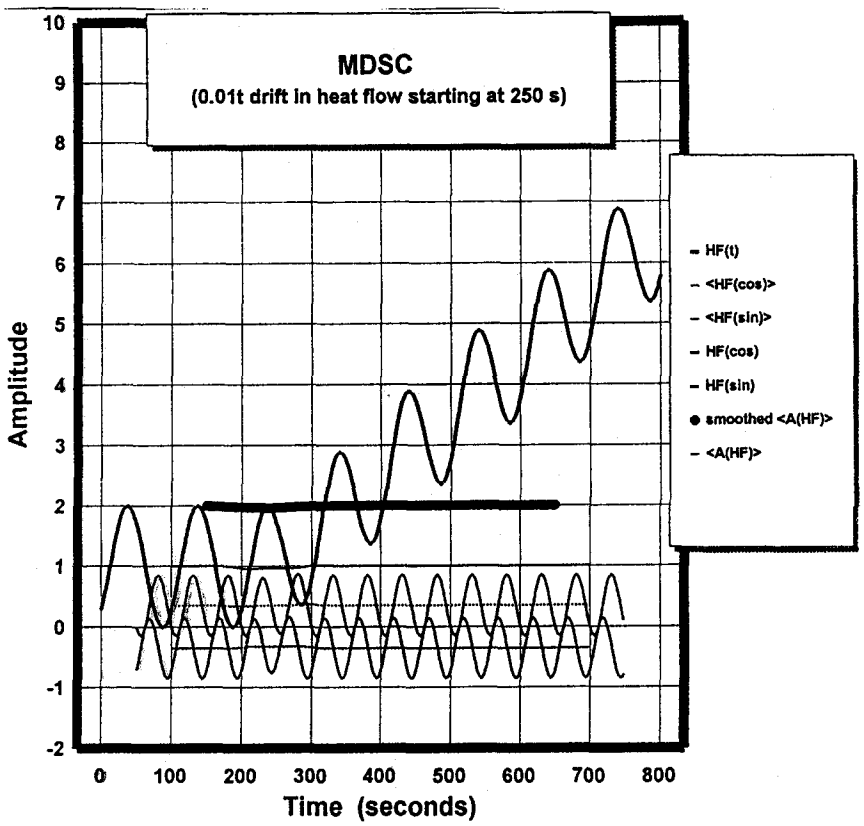

Fig. 4 Similar analysis as in Fig. 1, but with a strong heat-flow drift starting at 250 s. Note that for clarity the smoothed $\langle A_{HF} \rangle$ has been moved upwards by one unit. The HF_{sin} is the middle sinusoidal curve

with position and size of spikes reveals that: 1. The total heat flow $\langle HF(t)\rangle$ gives, naturally, always the proper sum. 2. Spikes during the negative portion of the modulation cycle give a negative contribution, and spikes during the positive portion, give a positive contribution. 3. The quantitative contribution to $\langle A_{HF}(t)\rangle$ varies. It is twice the actual amount at the maxima and minima of $HF(t)$ and goes through zero at the points of inflection. The contributions to $\langle HF_{sin}(t)\rangle$ and $\langle HF_{cos}(t)\rangle$ vary with the phase angle δ.

Figure 3 shows the effect of a 50% jump in heat flow that continues to the end of the experiment. The full effect of this large change in heat flow is visible in the total heat flow $\langle HF(t)\rangle$, while the reversing heat flow shows, as expected, no effect beyond the $\pm 1.5\ p$ modulation period. Within this narrow time period, however, positive or negative contributions may occur, depending on the phase of the heat flow when the change occurs. In both, the spike and abrupt change in heat flow, high-frequency harmonics would show in a Fourier series that describes the actual heat flow. By omitting all higher terms in the MDSC analysis, their contributions

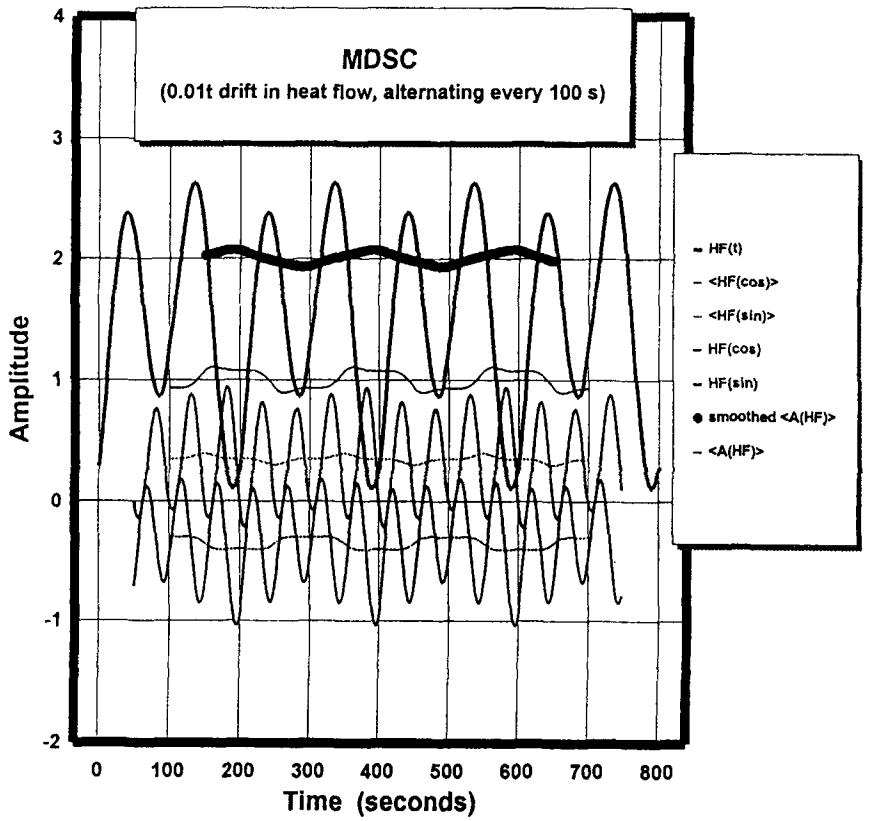

Fig. 5 Similar analysis as in Fig. 4, but with an alternating heat-flow drift throughout the simulation. Note that for clarity the smoothed $\langle A_{HF}\rangle$ has been moved upwards by one unit. The HF_{sin} is the middle sinusoidal curve

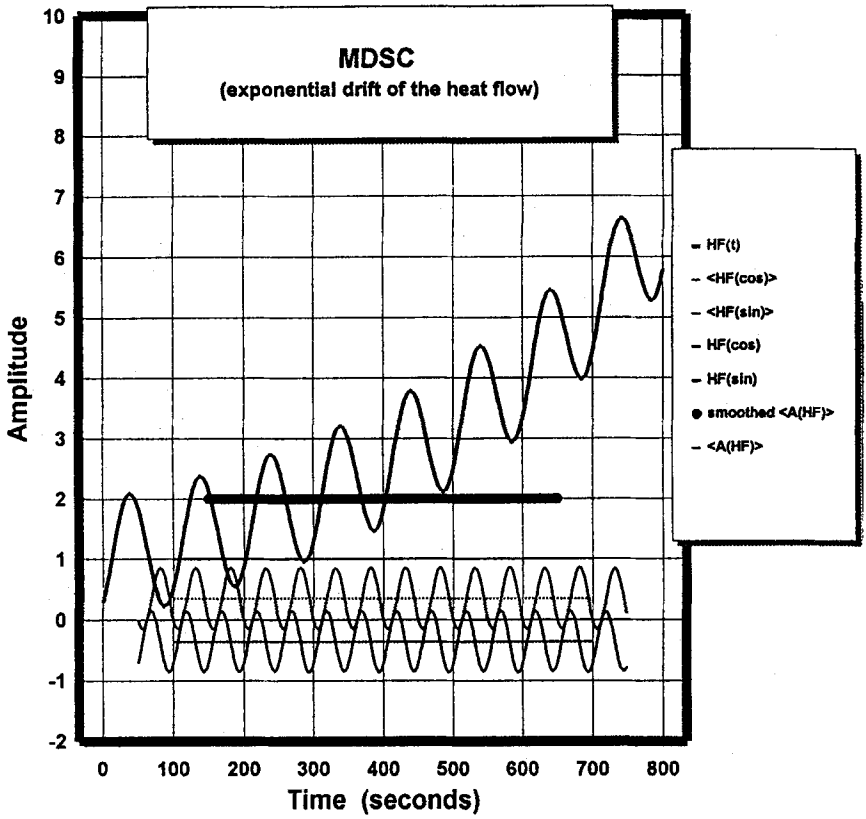

Fig. 6 Similar analysis as in Fig. 4, but with an exponentially increasing heat-flow drift throughout the simulation. Note that for clarity the smoothed $<A_{HF}>$ has been moved upwards by one unit. the HF_{sin} is the middle sinusoidal curve

are not accounted for. The simplified averaging in Eq. (10) keeps all Fourier components that average to zero over one cycle, p, as part of the reversing heat flow, causing the small errors for any abrupt change. If changes of this nature are present or expected, a simulation of the results with the present method may help in assessing the (small) error.

Figure 4 is the simulation of a continuously increasing heat flow, starting at 300 s. Such behavior may be seen if a sample experience either a continuously increasing loss of mass by evaporation, or an accelerating chemical reaction. As has been illustrated frequently, measurement of the reversing heat flow, and thus heat capacity, is feasible under such circumstances. The large amount of nonmodulated heat effect is effectively separated. Again, however, a small effect at the sharp onset is visible, stretching over the three averaged modulation cycles. Its value is, as before, dependent on the phase of the modulation and sharpness of the onset of the effect. Simulating the same drift as in Fig. 4 with reversing direction every 100 s,

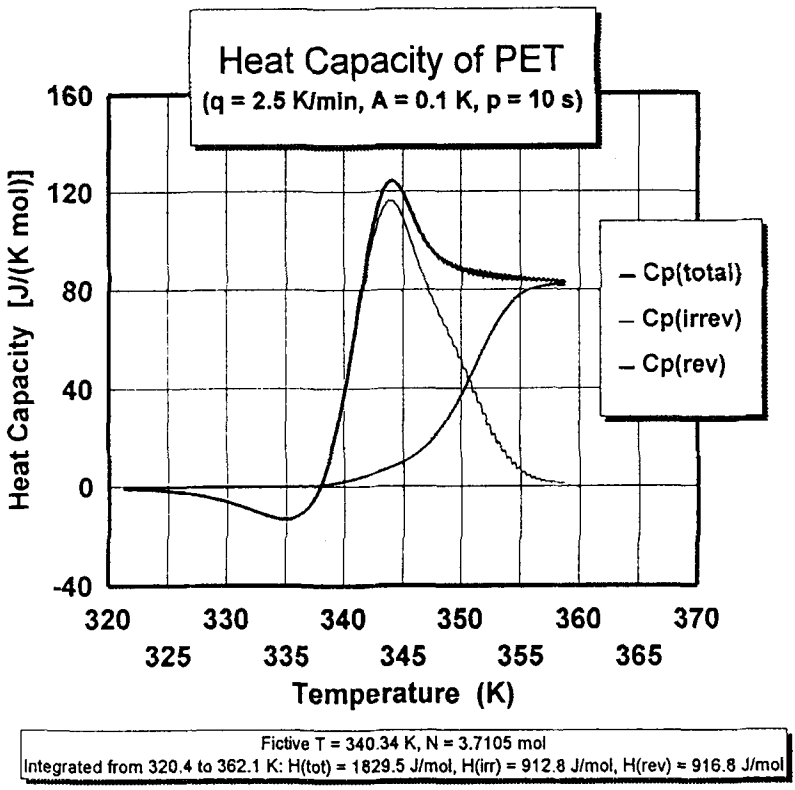

Fig. 7 Use of the spread-sheet analysis to analyze the time effects at the glass transition of poly(ethylene terephthalate) PET. For details see Refs [7, 8]

gives the results in Fig. 5. The added heat effect reaches 100% at each reversal, while the error in modulation amplitude in the smoothed $\langle A_{HF} \rangle$ is only about ±7%.

As a final example the same additional heat flow as in Fig. 4 is introduced more gradually, using an exponential increase that also reaches 5.5 at 800 s. Figure 6 gives the result. In this case that may be closer to reality, the effect on the smoothed $\langle A_{HF} \rangle$ is truly insignificant. Figures (3) to (6) show also the importance of and reasons behind the commonly proclaimed rule that several modulations must span a transition to be studied by MDSC.

Once the erroneous effects and lags due to thermal conductivity have been eliminated by proper choice of modulation, mass, and underlying rates, it is also possible to study actual kinetic effects in the sample, as is shown in more detail in the discussion of the glass transition [7, 8]. Figure 7 shows such an analysis of the heat capacity in the glass transition region making use of a similar spread sheet as in Table 1 for poly(ethylene terephthalate) with parameters derived from quasi-isothermal MDSC. The (negligible) influence of higher harmonics and the separation of reversing effects from nonreversing is possible.

Conclusions

A simple spread-sheet method is introduced for the simulation of MDSC measurements. It shows the limits of the chosen analysis methods and is a good learning tool to fine-tune ones experimental technique. Furthermore, it aids greatly in the separation of heat-flow and kinetic effects due to sluggish response of the sample itself.

* * *

This works was supported by the Division of Materials Research, National Science Foundation, Polymers Program Grant # DMR 90–00520 and Oak Ridge National Laboratory, managed by Lockheed Martin Energy Research Corp. for the U.S. Department of Energy, under contract number DE-AC05-96OR22464. Support for instrumentation came from TA Instruments, Inc. and research support was also given by ICI Paints, Exxon Res. and Eng. Co., and Shell Development Co.

'The submitted manuscript has been authored by a contractor of the U.S. Government under the contract No. DE-AC05-96OR22464.

Accordingly, the U.S. Government retains a non-exclusive, royalty-free license to publish, or reproduce the published form of this contribution, or allow others to do so, for U.S. Government purposes.'

References

1 M. Reading, Trends in Polymer Sci., 8 (1993) 248.
2 A. Hensel, J. Dobbertin, A. Boller, J. E. K. Schawe and C. Schick, J. Thermal Anal., 46, (1996) 935; J. E. K. Schawe, Thermochim. Acta, 260 (1995) 1.
3 B. Wunderlich, Y. Jin and A. Boller, Thermochim. Acta, 238 (1994) 277.
4 Y. Jin, A. Boller and B. Wunderlich, in Proc. 22nd NATAS Conf., 1993; and A. Boller, Y. Jin, and B. Wunderlich, J. Thermal Anal., 42 (1994) 307.
5 B. Wunderlich, A. Boller, I. Okazaki and S. Kreitmeier, Thermochim. Acta, 282/283 (1996) 143.
6 A. Boller, C. Schick and B. Wunderlich, Proc. 23rd NATAS Conf., J. B. Enns, editor, pp. 464–469 (1994). Full paper Thermochim. Acta, 266 (1995) 97.
7 A. Boller and B. Wunderlich, Proc. 24th NATAS Conf., S. A. Mikhail, Ed. pp. 136–141 (1995). Submitted as two papers: B. Wunderlich, A. Boller, I. Okazaki and S. Kreitmeier, Ref. 5, above; and A. Boller, I. Okazaki and B. Wunderlich, Thermochim. Acta 284 (1996) 1.
8 L. Thomas and B. Wunderlich, Thermochim. Acta, submitted (1996).
9 WWW (Internet), URL: http://funnelweb.utcc.utk.edu/~athas.
10 B. Wunderlich, 'Thermal Analysis,' Academic Press, Boston, 1990.